Sociedad Mexicana de Ingeniería Mecánica
Fecha de recepción: 10-04-2021
Fecha de aceptación: 20-05-2021

INGENIERÍA MECÁNICA
TECNOLOGÍA Y DESARROLLO
Vol. 7 No. 2 (2021) 017 - 024

Design of an automotive subframe by topological optimization

Diseño de un subchasis automotriz por medio de optimización topológica

[1]Vázquez-Vázquez V.A., [1]Velázquez-Villegas F., [2]Ascanio G.,
[1]Cuenca-Jiménez F., [1]Zepeda-Sánchez A., [1]Yáñez-Valdez R.
[1]Centro de Diseño Mecánico e Innovación Tecnológica
Facultad de Ingeniería, Universidad Nacional Autónoma de México
[2]Instituto de Ciencias Aplicadas y Tecnología
Universidad Nacional Autónoma de México

Abstract

The subframe is one of the heaviest parts in an automobile and, at the same time, it is one of the most rigid. Mass reduction in automobiles has become a design requirement to improve energy efficiency, which is why lightweight structures are required. In this work the front subframe of a generic automobile is designed applying topological structural optimization. The objective is to determine the optimal distribution of the subframe mass, which maximizes stiffness and reduces weight. General bump, sudden turning, acceleration, and abrupt braking load cases are considered. After adaptation for manufacture, the generated subframe could be made of steel or aluminum, weighing less than 20 kg and 7 kg, respectively. It means significant differences in comparison with conventional subframes, which weigh between 10 kg and 25 kg.

Resumen

El subchasis es una de las partes más pesadas en un automóvil y, al mismo tiempo, es una de las más rígidas. La reducción de masa en automóviles se ha convertido en un requerimiento de diseño para mejorar la eficiencia energética, por lo cual estructuras ligeras son requeridas. En este trabajo el subchasis frontal de un automóvil genérico es diseñado aplicando optimización estructural topológica. El objetivo es determinar la distribución óptima de masa en el subchasis, la cual maximiza la rigidez y reduce el peso. Son considerados los escenarios de carga bache general, giro repentino, aceleración y frenado abruptos. Después de la adaptación para manufactura, el subchasis generado puede ser fabricado de acero o aluminio, pesando menos de 20 kg y 7 kg, respectivamente. Esto se traduce en diferencias significativas en comparación con subframes convencionales, los cuales pesan entre 10 kg y 25 kg.

Keywords:

Vehicle mass reduction, subframe optimization, Lightweight vehicle structure, Topological optimization, Stiffness maximization

Palabras clave:

Reducción de masa en vehículos, optimización de subchasis, estructuras ligeras de vehículos, optimización topológica, maximización de rigidez

Introduction

Security and comfort systems in the automobile imply significant increases in weight, fuel consumption and pollutant emissions. From 1985 to 2005, for example, the weight of compact vehicles has increased up to 40% [1]. Therefore, weight reduction of the structure is very important in the automotive industry. Nowadays weight reduction strategies are to minimize components and subsystems size, increase stiffness designing complex transversal sections, new manufacture and union processes, selection of materials with high strength-weight ratio and optimization of structural components [2]. For the last one, an option is to apply topological optimization to design light structures whose stiffness-weight ratio is maximized.

Some examples of applying topological optimization are the following. In 2011 Wight [3] worked in optimizing the suspension uprights of a racecar, reaching 40% mass reduction and 25% stiffness increase maintaining stresses under 220MPa. In the same year, Costi [4] presented a work where several characteristics of the hood substructure of a Ferrari F458 Italia were improved; while stiffness increased about 5% weight reduced 12%. Another case is described in Cavazzuti's paper [5], where the conceptual design of the entire structure of a subcompact vehicle was optimized.

The subframe is the heaviest component of the mechanical control system in an automobile, therefore, it is a perfect candidate to reduce structural weight. The weight of commercial subframes varies from 10 kg to 25 kg [6]. This part can be topologically optimized, if it is considered as a single part subjected to multiple load cases, to generate a new conceptual design for it. In this work the following load cases were considered: general bump, sudden turning, acceleration, and abrupt braking; each of them was applied as a static load affected by a dynamic factor.

Method

Topological optimization is a method used to generate the best conceptual solutions for structural design problems. The main idea is to optimize the material layout in a defined design domain for given boundary conditions, load cases and requirements. The topological optimization problem implies that the design domain is modeled as a mesh of finite elements. A relative density (ρ) is associated to each finite element and is used as design variable, which is individually modified according to the performance level of each element [7].

In general terms, the lower the strain energy, the higher the stiffness of a structure. In a design domain meshed with finite elements, the individual stiffness of every element can be defined as a function of its density, so the optimization can be driven by varying ρ along the domain in a discrete way. Mass constraint is established to control the minimal and maximal mass in the structure. This is important because mass variation can produce disconnected regions and, therefore, unfeasible solutions.

The general topological optimization problem statement is described as follow:

$$\min \int_{\Omega} \frac{1}{2}\sigma \cdot \varepsilon \, d\Omega; \text{ subject to } \begin{cases} \rho \in [0,1] \\ m_{cmin} \le \int_{\Omega} \rho d\Omega \le m_{cmax} \left(mass\, constraint\right) \\ \nabla \cdot \sigma + \vec{F} = 0 \left(balance\ ecuation\right) \\ \sigma = C \cdot \varepsilon \ \left(constitutive\ ecuation\right) \end{cases} \tag{1}$$

where Ω is the design domain, σ and ε are stress and strain distributions, respectively, m_{cmin} and m_{cmax} are the minimum and maximum mass allowed, $\vec{F}$ represents the boundary conditions, and $\boldsymbol{C}$ is the stiffness tensor [8].

It is important to point that the conceptual solutions, although optimal, may be unfeasible for manufacturing. This issue can be overcome adding manufacturing constraints to the optimization process; however, this may be insufficient because of the geometric complexity. In these cases, the solution must be adapted, as a final step, to obtain a design that satisfies practical manufacturing requirements.

Case study

Figure 1 shows the subframe considered for being optimized, interacting with other vehicle parts. Figure 2 shows the points where the part is supported, it means the positions where the boundary conditions were applied to the reference model. This model was obtained from the Crash Simulation Vehicle Models Database of the National Highway Traffic Safety Administration (NHTSA [9]).

Based on this subframe model, the design domain shown in Figure 3 was generated. It is worth mentioning that the geometry of the protrusions was arbitrary because they were only used to connect the boundary conditions and restrictions to the design domain.

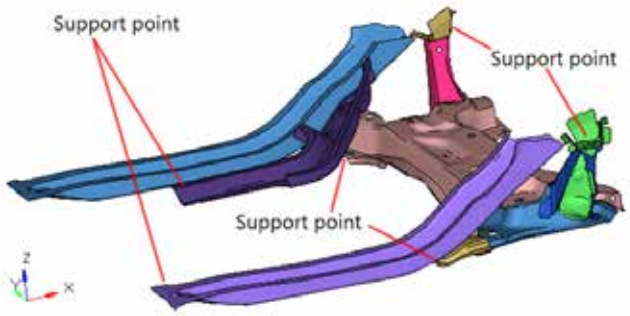

Figure 2 Support points in the main frame [10]

Load cases.

During the phase of conceptual design, static loads, and dynamic amplification factors (acceleration factors) were used to model the most critical load cases without the complexity

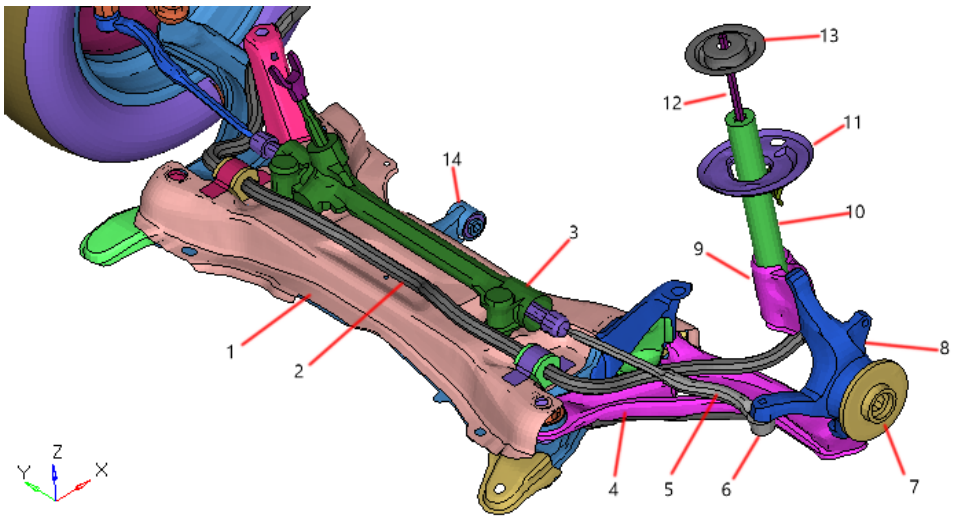

1.- SUBFRAME
2.- Stabilizer bar
3.- Steering mechanism
4.- Control arm
5.- Steering palier
6.- Spherical joint
7.- Cube
8.- Coupling
9.- Support assambly
10.- Shock absorber tube
11.- Top bracket suspension
12.- Spring
13.- Bottom bracket suspensión
14.- Motor support joint

Figure 1 Subframe interacting with other parts [10]

EDICIÓN DIGITAL
ISSN 2448-5837

of dynamic loads. In this way, the actual behavior of the subframe was estimated. Usually, the loads transmitted to the subframe are defined in terms of acceleration factors that affect the static forces; therefore, they are independent of the vehicle, and they can be easily modified [11, 12].

At the early design stage, the main interest focuses on instantaneous strength. Therefore, at this stage, it could be assumed that 'if the structure can resist the (rare) worst possible loading which can be encountered, then it is likely to have sufficient fatigue strength' [12]. The load cases considered in this work were general bump, sudden turning, acceleration, and abrupt braking. Table 1 shows the acceleration factors for standard load cases used in vehicle design according to ISO-7975:2006 "Passenger cars – Braking in a turn – Open loop test procedure" [13].

The static weight distribution on each wheel was calculated to determine the forces affecting the subframe, according to the relations shown in Figure 4, where l is the wheelbase, l_f is the distance from the gravity center (GC) to the front wheels, h is the high of GC, g is the gravity acceleration, and m_t the total mass [14]. For the vehicle in this work: g=9.8 and m_t=1078 Kg. Therefore, the mass in the front wheels (m_{fw}) was 647 Kg (60% of m_t) and 431 Kg in the rear wheels. The forces for each load case were calculated multiplying the static forces by the acceleration factors (Table 1), and oriented according to the coordinate system shown in Figure 5.

Table 1 Standard load cases for structural analysis in vehicles [13]

Standard load cases – Structural Strength	Acceleration factors		
	x	y	z
Stationary Vehicle	0.00	0.00	0.00
General Bump	2.50	2.50	3.00
Cornering	0.00	±1.25	1.00
Braking	-0.75	0.00	1.00
Braking and cornering	-0.75	0.75	1.00
Acceleration	-0.50	0.00	1.00
Acceleration and cornering	-0.50	0.50	1.00

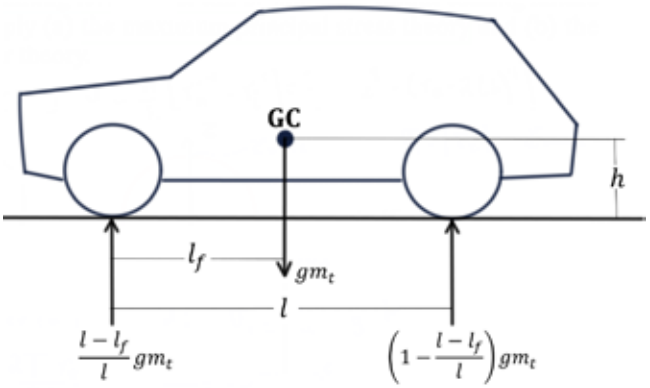

Figure 4 Static loads on the automobile [14].

General bump

This load case was defined as the superposition of longitudinal, vertical, and lateral bump load cases. The longitudinal, lateral, and vertical acceleration factors were, respectively, -2.5, 2.5 and 3 according to Table 1. The calculated force components on each front wheel that suffers general bump were: F_x=-7.90 *KN*, F_y=7.90 *KN* and F_z=9.48 *KN*.

Cornering.

When a vehicle is driven into a sharp curve, the outer wheels experience greater forces than those in the static case because of the centrifugal effect. In the most critical situation, the inner wheels experience a third of the static vertical forces, while the outer wheels support five thirds of those forces, being the total vertical force for this load case twice the static force [13]. That means F_z=1.06 *KN* in the front inner wheel and F_z=5.28 *KN* in the front outer wheel. Considering the acceleration factor in Table 1, i. e. 1.25, the lateral force in each wheel was F_y=1.32 *KN* in the inner wheel and F_y=6.60 *KN* in the outer one. It is obvious that this load case should be considered on both sides, not simultaneously, because a vehicle is driven to the left or to the right.

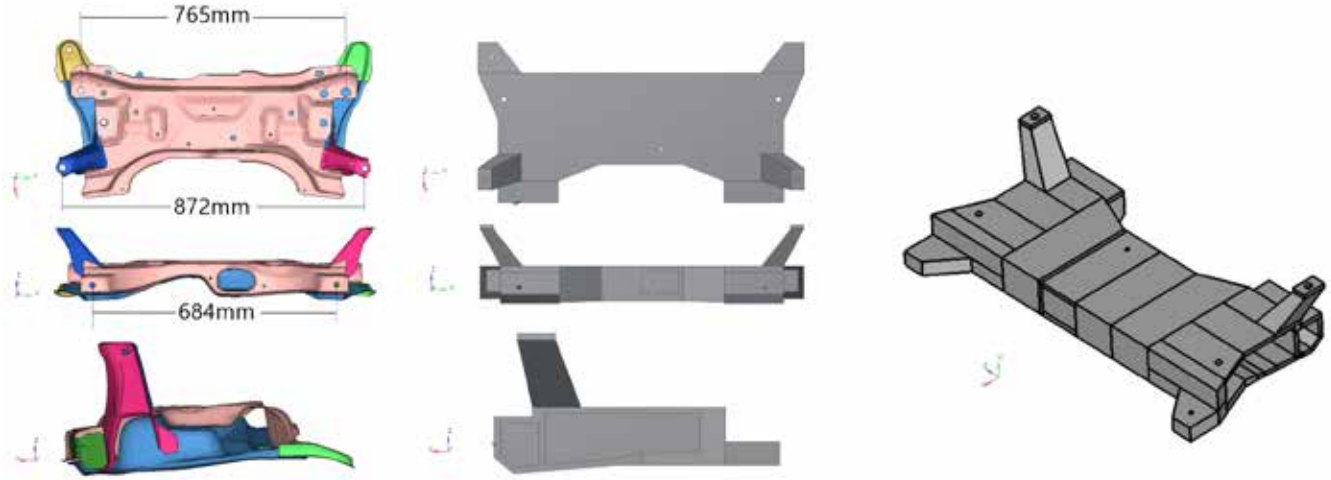

Figure 3 Design domain generated from the original model.

ISSN 2448-5837

EDICIÓN DIGITAL

Braking and Acceleration.

Due to the dynamic effect of braking, the mass supported by the front wheels changes according to the equation (2), where m_{fwb} is the mass supported during braking by the front wheels and μ is the frictional coefficient between the ground and the wheels. A very common value of μ, during braking, is 0.9 [13]. Therefore, knowing that m_{fwb}=859 *Kg*, for each wheel the vertical force is F_z=4.21 *KN* and, considering the acceleration factor for braking, the horizontal force was F_x=-3.16 *KN*.

$$m_{fwb} = \frac{\left(l - l_f + \mu h\right)}{l} m_t \tag{2}$$

According to Table 1 when a vehicle suddenly accelerates longitudinal forces appear over the wheels, whose magnitude is a half of the vertical forces, hence F_z=3.17 *KN* and F_x=-1.59 *KN*.

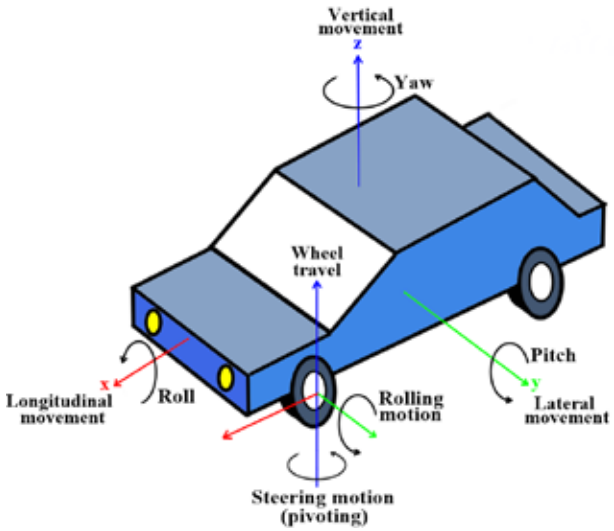

Figure 5 Coordinate system on the automobile [13].

Finite element model and constraints

A fine lineal tetrahedral mesh was used, with an element size of 5 mm, which was adequate to represent accurately the design domain and to generate good quality results. Steel AISI 52100 (Young's modulus 200GPa, yield stress 280 MPa, density 7890 Kg/m^3) was considered as a first option of material. The initial mass of the design domain was 155 kg. The finite element model, the analysis and the optimization were developed in the Altair-Hyperworks software [15,16].

The forces produced by the roll bar and the steering were considered as negligible because their magnitudes and effects over the subframe are much smaller than the forces produced by the control arm. This component was simplified as a rigid frame that transmits forces to the joints in the subframe. In other hand, the joining zones between the subframe and the main structure were considered as constrained surfaces (Figure 6). Each load case was applied through the control arm. As an example, Figure 7 shows the load case General bump over the right wheel.

Optimization results

In the optimization process, the following guidelines were considered. In first place, the optimal subframe should be light, therefore, the mass of the design domain was reduced as much as possible. At the same time, the subframe should be rigid enough to support all the non-simultaneous load cases. Therefore, stiffness was maximized. Another important constraint needed in the subframe was symmetry because driving occurs in both directions right and left. After several iterations, the optimal structure reached a mass of 7.5 kg (Figure 8). Obviously, this optimal structure was just a conceptual solution to the subframe because it cannot be manufactured directly; so, an adaptation process was required, in which this conceptual solution was modified to satisfy manufacture requirements.

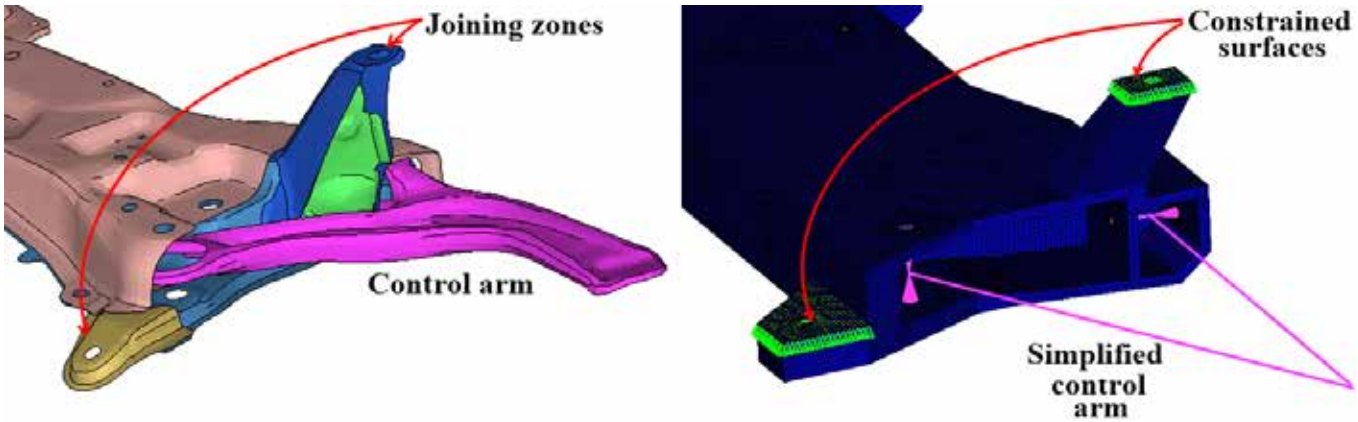

Figure 6 Control arm simplified as two bars rigid frame and constrained surfaces.

EDICIÓN DIGITAL
ISSN 2448-5837

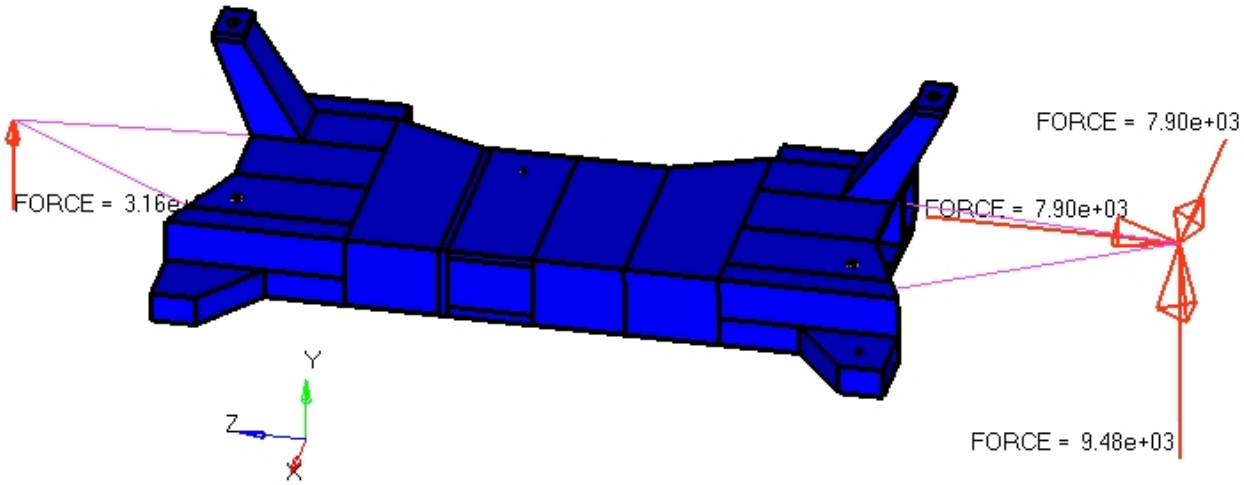

Figure 7 General bump over the right wheel.

Adaptation process

The structure was divided in three different parts to facilitate the adaptation process (Figure 9), which had two phases.

First phase.- the parts were modified by changing thickness and simplifying the geometry of cavities, some of them were omitted because they were very small. Besides, symmetry was applied to the geometry because it is a required characteristic in the subframe. After this process, the subframe structure shown in Figure 10 was obtained.

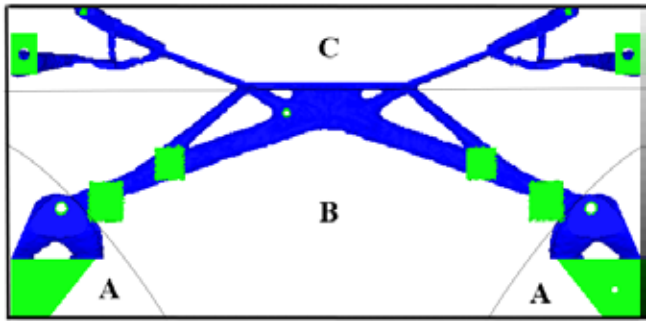

Figure 9 Sections in the conceptual solution.

Second phase.- the structure was modified based on the stress level. In this iterative phase the load cases were applied to the new structure to determine zones where the stress level was high. These zones were modified by including or varying chamfers, fillets, and thickness to eliminate stress concentrators and to generate a robust enough structure that supports all the load cases. In this phase, section A and C suffered the most drastic modifications because they presented several stress concentrators. These were eliminated by implementing fillets (Figure 11). In Figure 12 the stress distribution in the final subframe structure is shown for general bump load case, which is the most critical of all of them. The maximum von Mises equivalent stress occurred in the fillets around the holes in section A (187 MPa). Additionally, for all load cases, the subframe was a fully stressed structure with a low overall stress level.

Manufacture proposal.

Although the first option was steel AISI 52100, for this early design phase, aluminum alloys were also worth considering, as indicated by the Standard BS EN 573-1:2004 [17]. It recommends these alloys for producing subframe and other structural elements in the automotive industry, because of their high strength-weight ratio and their molding ease. The EN AW 6063 alloy was chosen, whose mechanical properties are: density 2686 Kg/m^3, Young's Module 72.5 GPa, Poisson

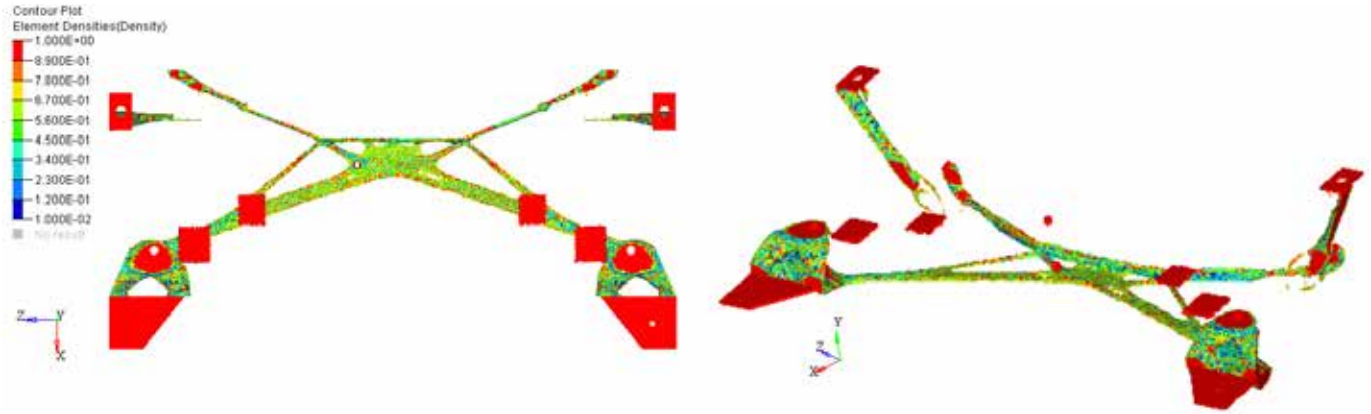

Figure 8 Subframe structure after the optimization process.

ISSN 2448-5837

Edición digital

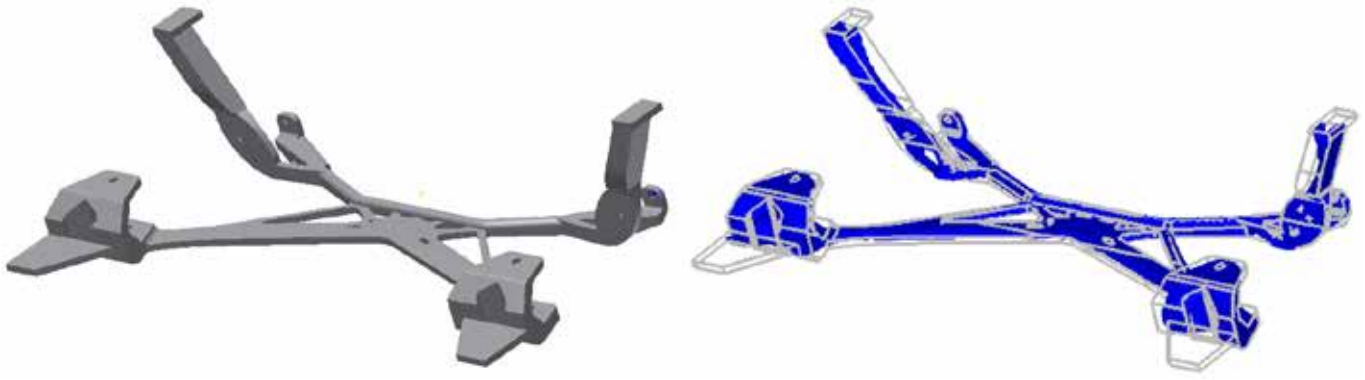

Figure 10 Adapted subframe geometry after the first phase of adaptation in comparison with the topologically optimized geometry.

ratio 0.33, yield stress according to the type of tempering: 130-145 MPa (T4), 145-190 MPa (T5) and 200-245 MPa (T6). Based on the maximum equivalent stress for the worst case (~187 MPa), the EN AW 6063 T6 alloy was considered for manufacturing the subframe.

The manufactured chassis was conceived as the union by welding of several parts. For the four connecting parts (Figure 13), molding and machining processes were considered. During the adaptation phase, the central body of the subframe was conceived as a plane body with symmetrical holes. In Figure 14 is shown the central body as the union of a folded tube and a machined plate, both made of EN AW 6063 T6 alloy.

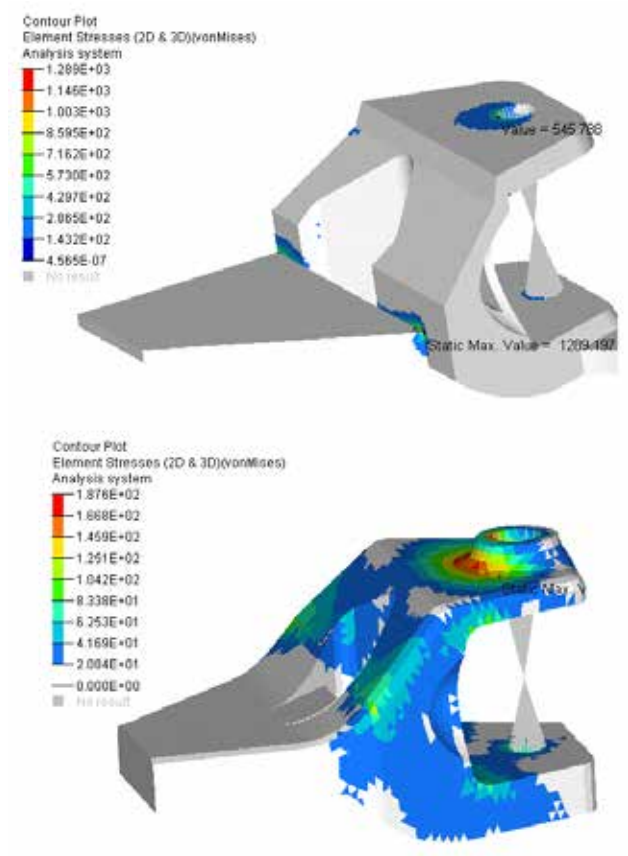

Figure 11 Left: Part in the section C after the first adaptation phase. Right: Final geometry after the second adaptation phase.

Made of steel the subframe would weigh 19.6 kg (up to 22% less compared to commercial options). Made of aluminum it would weigh 6.7 kg (up to 73% less).

MIG welding process was considered as a first option because it is unexpensive. Linear friction welding process could be an excellent alternative to avoid filler metal. The subframe is integrated as the Figure 15 shows.

Conclusions.

The design of a subframe, applying topological optimization and an adaptation process, was presented in this work. The most critical loads were considered as static load cases based on the automobile weight and dynamic amplification factors. In this way the dynamic effects were estimated. Based on the maximum von Mises equivalent stress, steel AISI 52100 and aluminum alloy 6063 T6 were considered as raw material for the subframe. Compared to commercial options, the designed subframe was up to 22% lighter (for steel) or up to 73% lighter (for aluminum), without sacrificing stiffness. In addition, it is a fully stressed structure with a low overall stress level. The adaptation process was a critical phase for the design due to the optimal distribution of mass should be preserved, while manufacture constraints should be considered. Up to today there is not a simple method to the adaptation process, therefore it strongly depends on the experience of structural designers and, consequently, it requires a long time. However, given the benefit, the effort is worth it.

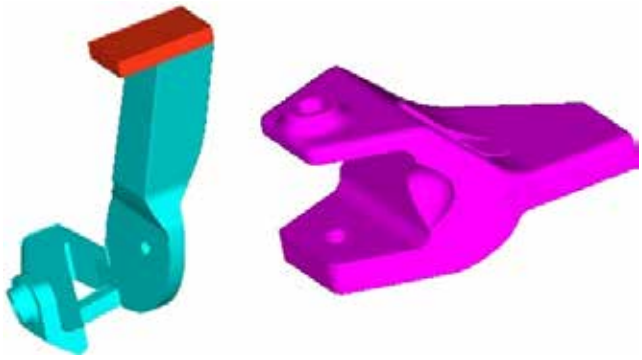

Figure 13 Parts connected to the main structure.

EDICIÓN DIGITAL

ISSN 2448-5837

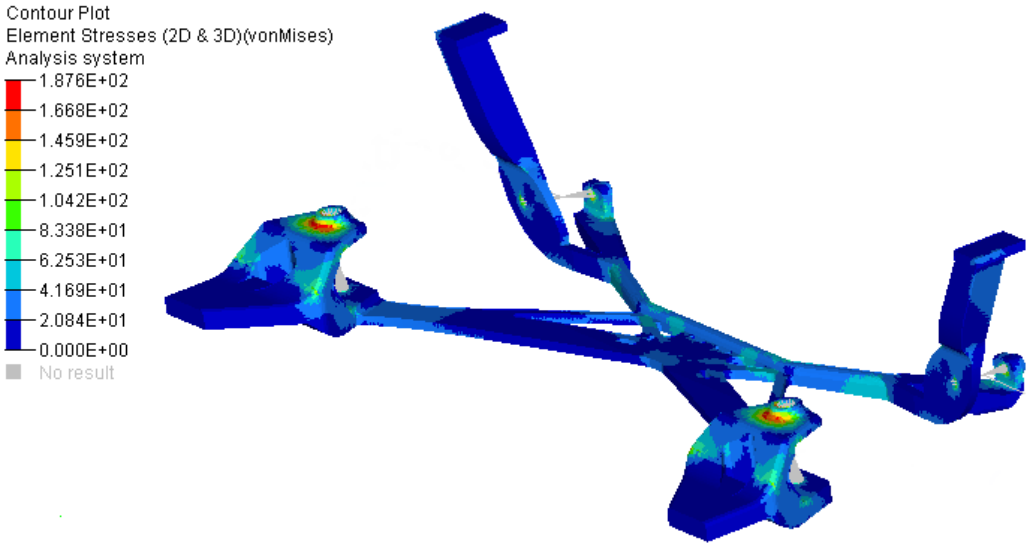

Figure 12 Stress distribution in the final subframe for the worst case (general bump).

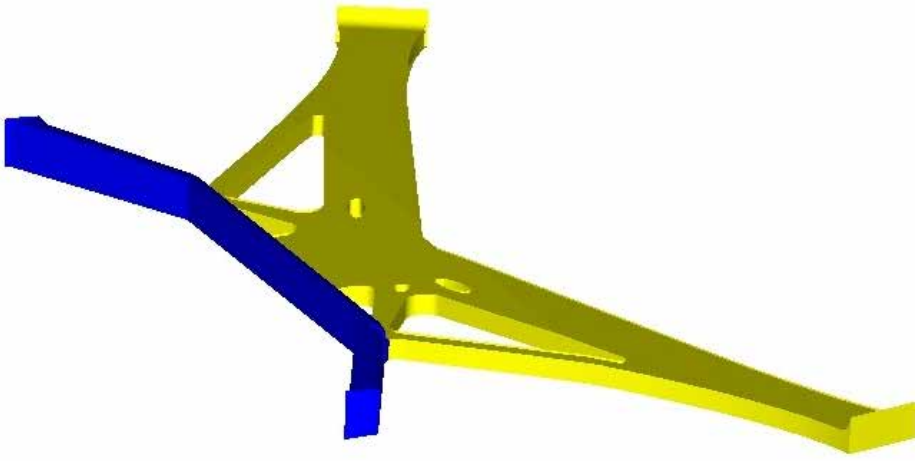

Figure 14 Central body.

Acknowledgment

This work was supported by DGAPA-UNAM [PAPIIT IN113315].

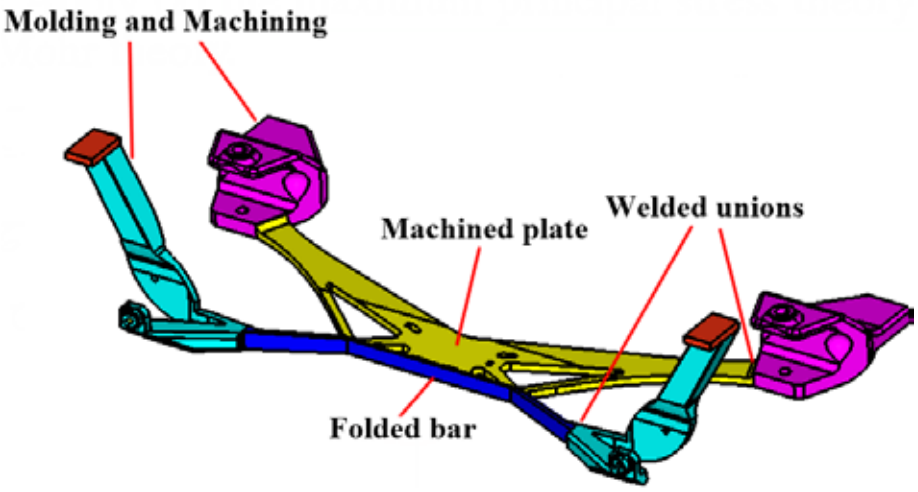

Figure 15 Final subframe

ISSN 2448-5837

EDICIÓN DIGITAL

References

[1] Zengen, K.-H. *Aluminum and Energy in the EU*. European Aluminum Association. Brussels, 27 March 2006. Information source: Jaguar.

[2] Grujicic M., Arakere G, Sellappan V, Ziegert J.C. and Schmueser D. *Multi-disciplinary Design Optimization of a Composite Car Door for Structural Performance, NVH, Crashworthiness, Durability and Manufacturability*. Multidiscipline Modeling in Materials and Structures 2009, Vol. 5 Issue: 1, pp.1-28,

[3] Wight B. *Topology Optimization of Racecar Suspension Uprights*. Online Referencing, https://www.luxonengineering.com/pdf/asme_presentation.pdf (2008, accessed December 2017).

[4] Costi D., Torricelli E., Splendi L. and Pettazzini M. *Optimization Methodology for an Automotive Hood Substructure (Inner Panel)*. In Proceedings of the World Congress on Engineering Vol III, London, U.K., July 6-8 2011, pp 1-4.

[5] Cavazzuti M., Costi D., Baldini A. and Moruzzi P. *Automotive Chassis Topology Optimization: a Comparison between Spider and Coupé Designs*. In Proceedings of the World Congress on Engineering Vol III, London, U.K., July 6-8 2011, pp 1-5.

[6] European Aluminium. *Aluminium Automotive Manual - Applications- Chassis & Suspension - Subframes*. 2011(https://www.european-aluminium.eu/resource-hub/aluminium-automotive-manual/)

[7] Xie Y. M. and Steven G. *Evolutionary Structural Optimization*. London: Springer-Verlag, 1997.

[8] Olason A and Tidman D. *Methodology for Topology and Shape Optimization in the Design Process*. Master's Thesis, Chalmers University of Technology, Sweden, 2010.

[9] National Highway Traffic Safety Administration. *Crash simulation vehicle models*. Online Referencing https://www.nhtsa.gov/crash-simulation-vehicle-models (undated) accessed January 2018.

[10] Fernandez J. *Simulación virtual de una suspensión McPherson en un entorno VRML*. Thesis, Universidad Carlos III, España, 2011.

[11] Heissing B. and Ersoy, M. *Chassis Components. In: Chassis Handbook Fundamentals, Driving Dynamics, Components, Mechatronics, Perspectives*. Springer Vieweg, 2011, pp 149-381

[12] Brown J.C., Robertson A.J. and Serpento S.T. *Motor Vehicle Structures: Concepts and Fundamentals*. Oxford: Butterworth Heinemann, 2002, p.14.

[13] Passenger cars -- *Braking in a turn -- Open-loop test method*. ISO 7975:2006. International Organization for Standardization, (April 2006)

[14] Reimpell J., Stoll H. and Betzler J. W. *Chasis and Vehicle overall. In: The Automotive Chassis: Engineering Principles*. 2nd ed. Oxford: Butterworth-Heinemann, 2002, pp 386-421

[15] Altair University, *Practical Aspects of Finite Element Simulation: A Study Guide*, 3rd ed. Michigan, 2015.

[16] Chapple A., Kemp M., Fisher K. and Willment T. *Evolutionary Design in Chassis Technology*, Altair Prouct Design 2011.

[17]Aluminium and aluminium alloys. Chemical composition and form of wrought products . Numerical designation system. Standard BS EN 573-1:2004. British-Adopted European Standard, (November 18, 2004)

EDICIÓN DIGITAL

ISSN 2448-5837